

# $\alpha$ -Cyclodextrin-Catalyzed Symmetry Breaking and Precise Regulation of Supramolecular Self-Assembly Handedness with Harata–Kodaka’s Rule

Wanwan Zhi,<sup>#</sup> Zhichen Pu,<sup>#</sup> Cheng Ma, Kaerdun Liu, Xuejiao Wang, Jianbin Huang, Yunlong Xiao,<sup>\*</sup> and Yun Yan<sup>\*</sup>

Cite This: <https://doi.org/10.1021/acsnano.1c06766>

Read Online

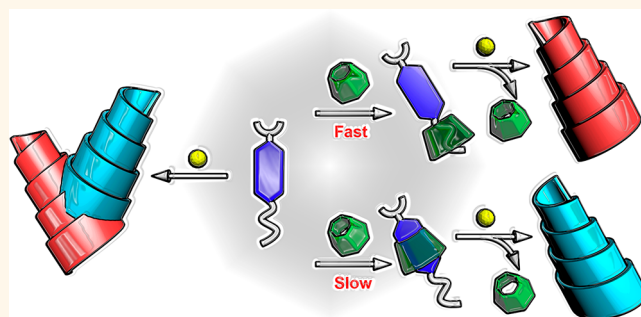
ACCESS |

Metrics & More

Article Recommendations

Supporting Information

**ABSTRACT:** Harata–Kodaka’s rule predicting the induced chirality of the guest molecules by cyclodextrins has been discovered in the 1970–1990s, yet its ability to control the supramolecular handedness of self-assembled structures has not been sufficiently recognized. Here we show that in a coordinating self-assembly system that is able to form racemic cone shells symmetry breaking occurs if the ligand is prethreaded into  $\alpha$ -cyclodextrin prior to metal ion addition, and the handedness of cone shells can be rationally manipulated by creating the two scenarios of the Harata–Kadaka rule through controlling the host–guest dynamics. Since the coordination complexes have strong self-assembling ability, the coordinating ligand would dethread from the cavity of  $\alpha$ -cyclodextrin but leaving the induced chirality to the coordinating self-assembly, thus catalyzing symmetry breaking. This work reveals that the dynamic factors such as concentration and molar ratio may play important roles in symmetry breaking at the supramolecular level. The current strategy provides a promising method for the symmetry breaking and manipulation of the handedness of self-assembled materials formed by achiral molecules.



**KEYWORDS:** symmetry breaking, Harata–Kodaka’s rule, host–guest dynamics, catassembly,  $\alpha$ -cyclodextrin

## INTRODUCTION

Symmetry breaking at various length scales in Nature remains a big mystery. In the past decades, people have endeavored a great effort to explore possibilities that might lead to chiral structures, particularly chiral supramolecular self-assembly generated from achiral molecules,<sup>1–3</sup> since this not only allows generating chiral materials with low cost but also sheds light on the origin of meso- and macro-scaled chirality in Nature. So far, people are able to trigger symmetry breaking of helical structures with chiral “generals”,<sup>4–6</sup> mechanical fields,<sup>7,8</sup> light,<sup>9–11</sup> heat,<sup>11</sup> metal coordination,<sup>12,13</sup> hydrogen bonding,<sup>14</sup> solvent manipulating,<sup>15,16</sup> space confinement,<sup>17–19</sup> or steric hindrance.<sup>20,21</sup> These diversified approaches have greatly broadened people’s horizons on the possible origin of supramolecular chirality. However, except for the approaches involving chiral general and mechanical fields, it still remains ambiguous to rationally regulate the handedness of the resultant self-assembled structure.

Cyclodextrins ( $\alpha, \beta, \gamma$ -CyD) are cyclic oligosaccharides composed of 6,7,8-D-glucopyranose units connected with 1,4-glycosidic bonds.<sup>22</sup> The cavity of cyclodextrins (CyD) is chiral, which can induce circular dichroism (ICD) for the achiral guest it accommodates.<sup>23</sup> In the 1970–1990s, Harata<sup>24,25</sup> and Kodaka<sup>26–28</sup> et al. figured out that for a guest with its chromophore inside the cavity of CyDs the dipole–dipole interactions between CyD and the chromophore would result in a positive ICD spectrum, if its electric transition dipole moment  $\mu$  is parallel to the main axis of CyD.<sup>24</sup> On the contrary, if the chromophore is outside of the cavity of CyDs, a

Received: August 6, 2021

Accepted: October 25, 2021

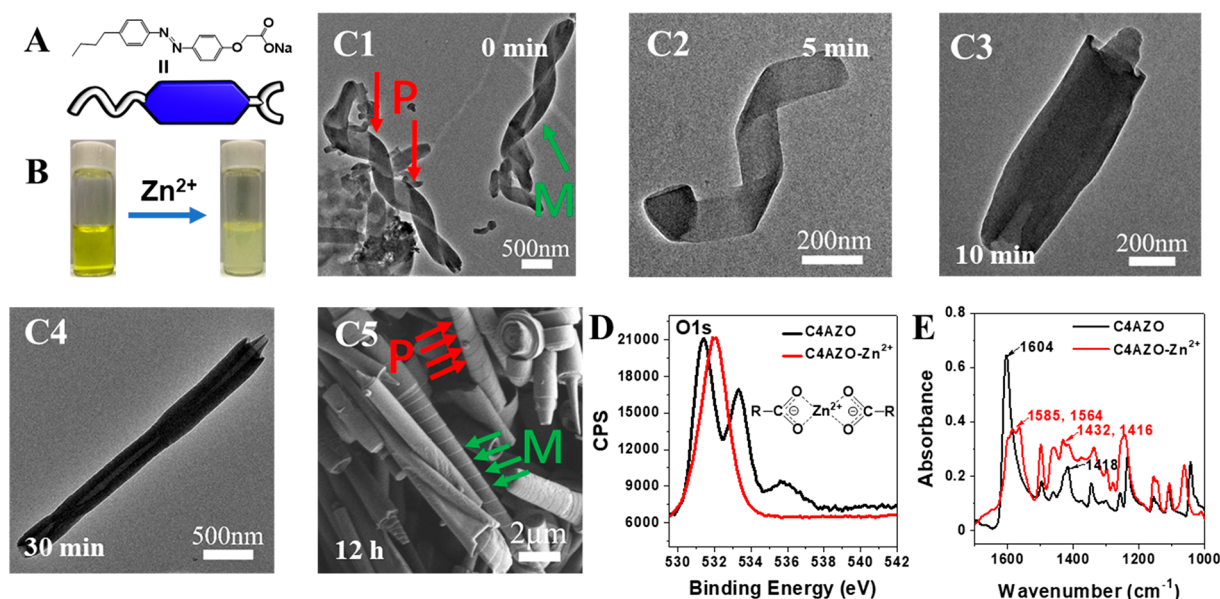
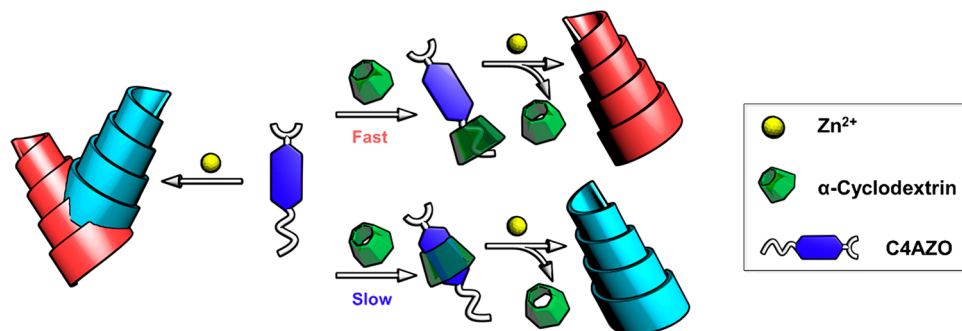


**Figure 1.** (A) Molecular structure of C4AZO and its schematic configuration. (B) Photographs of the aqueous solution of C4AZO and the suspension it forms with  $\text{Zn}^{2+}$  ( $\text{C4AZO-Zn}^{2+} = 0.5:0.25 \text{ mM}$ ). (C) Time-evolution images of the microtubular structures. (C1–C4) TEM images captured, respectively, on the timeline of 0 min, 5 min, 10 min, 30 min, and 12 h. Note that the two pictures in C1 were obtained from the same example. (C5) SEM image after 12 h of stabilization. (D) XPS measurement for the O 1s binding energy of C4AZO before and after coordination with  $\text{Zn}^{2+}$ . (E) FT-IR spectra of C4AZO before and after coordination with  $\text{Zn}^{2+}$ .

**Scheme 1. Illustration of the  $\alpha$ -Cyclodextrin-Catalyzed Symmetry Breaking of Coordinating Self-Assembly of  $\text{Zn}(\text{C4AZO})_2$  Cone Shells**



negative ICD should be expected.<sup>28</sup> In the past half century, the above Harata–Kodaka rule was extensively utilized to predict the absolute configuration of the achiral guest in the cavity of CyDs<sup>29–32</sup> but has never been considered in symmetry breaking in racemic self-assembled structures and controls the handedness of supramolecular structures.

Recently, people have recognized that some molecular self-assembled structures can be assisted by a “helper”.<sup>33,34</sup> Tian et al. suggested to use the term “catassembly” to refer to this process as “catalyzed assembly”.<sup>35</sup> In analogy to the role of catalysis in a chemical reaction, the “helper” participates in the self-assembling process but would not appear or exist as a negligible component in the final self-assembled structures, just like what catalysis does in a chemical reaction. It has been expected that catassembly would be an effective approach to obtain “state-of-the-art” self-assembled materials.<sup>36–38</sup> Considering that the occurrence of chiral molecular self-assembled structures with achiral molecules is usually under certain circumstances, we expect that catassembly could probably be a suitable strategy leading to symmetry breaking with rationally

designed handedness in a racemic self-assembling system. However, so far this scenario has not been demonstrated.

Herein, we report an unusual case of  $\alpha$ -cyclodextrin ( $\alpha$ -CyD)-catalyzed symmetry breaking in the racemic chemical cone shells self-assembled from the zinc salt of the alkyl azobenzene carbonate (Figure 1A). Upon controlling the host–guest dynamics through varying the host-to-guest ratio or the total concentration, we are able to selectively obtain the left- (*M*) or right-handed (*P*)  $\text{Zn}(\text{C4AZO})_2$  cone shells. The underlying physics is that the fast exchanging of C4AZO in and out of  $\alpha$ -CyD favors shallower threading of the butyl azobenzene carbonate in the cavity of  $\alpha$ -CyD, whereas the slow guest exchange favors a deeper threading (Scheme 1). According to Harata–Kodaka’s rule, these two scenarios generate a reverse ICD signal, which leads to cone shells with reverse handedness. The current work indicates that the factors influencing the self-assembling dynamics of critical molecules perhaps have a determinative role in deciding the supramolecular chirality in nature.

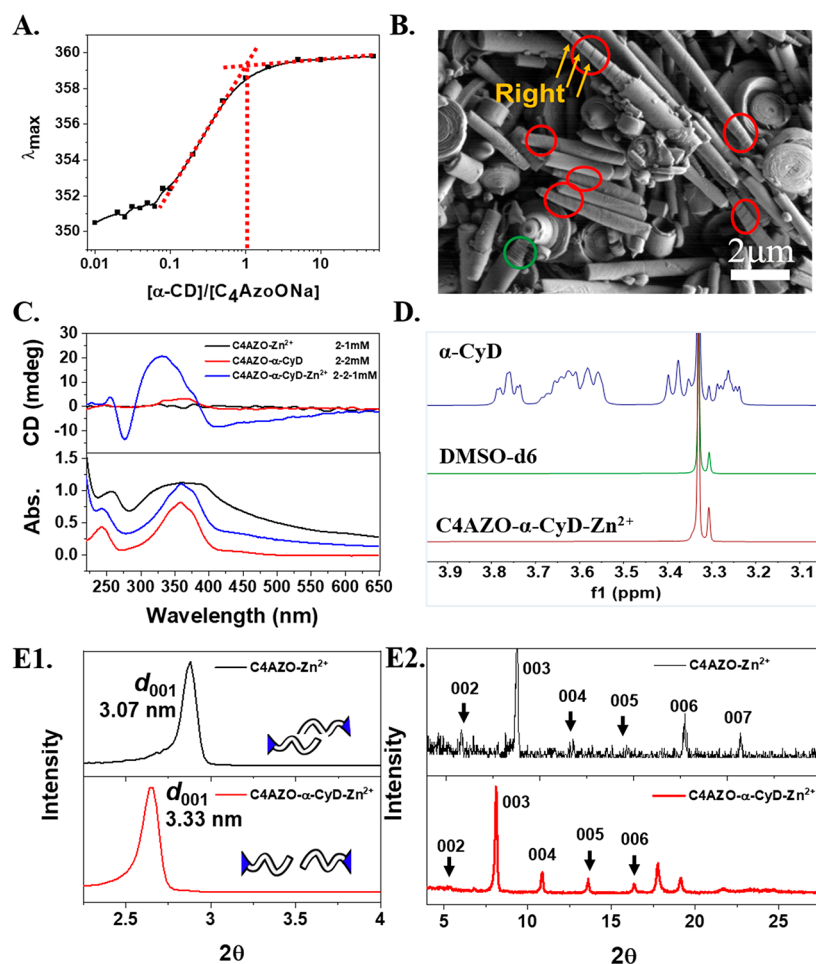


**Figure 2.** (A) Molecular structure and sizes of  $\alpha$ -CyD. (B) SEM image of the aggregates formed after adding  $\text{Zn}^{2+}$  into the solution of C4AZO- $\alpha$ -CyD ( $\text{C4AZO}/\alpha\text{-CyD}/\text{Zn}^{2+} = 2:2:1$  mM). Left- (*M*) and right-handed (*P*) cone shells are circled as green and red, respectively, to count their numbers, and the following picture is the same. (C) CD spectra that show the emergence of symmetry breaking. (D) NMR spectra of the C4AZO- $\alpha$ -CyD- $\text{Zn}^{2+}$  aggregates. The peaks that occur at  $\delta = 3.33$  ppm are from water absorbed by DMSO- $d_6$  solvent. (E) XRD spectra of C4AZO- $\text{Zn}^{2+}$  and C4AZO- $\alpha$ -CyD- $\text{Zn}^{2+}$  aggregates. (E1 and E2 represent the small and wide-angle part of the spectra, respectively. The insets in E1 illustrate how the butyl chains staggered in the bilayers of the racemic and *P*-chiral cone shells, respectively.)

## RESULTS AND DISCUSSION

**Formation of Racemic Spiral Cone Shells.** The achiral guest C4AZO (Figure 1A) was synthesized in our lab according to the literature.<sup>39</sup> UV-vis measurement suggests that this compound would undergo *trans*-to-*cis* isomerization under UV irradiation (Figure S1). Under visible light, the *trans*-isomer is about 66% according to  $^1\text{H}$  NMR measurements (Figure S2). In water, C4AZO molecules form irregular clusters around 10–50 nm (Figure S3). A turbid suspension was formed immediately after mixing the aqueous solution of C4AZO and zinc nitrate ( $\text{Zn}(\text{NO}_3)_2$ ) at the molar ratio of C4AZO- $\text{Zn}^{2+} = 2.0$  (Figure 1B), indicating the interaction between  $\text{Zn}^{2+}$  and C4AZO has formed a complex with strong self-assembling ability. The disappearance of the UV-vis feature for the *cis*-isomer (Figure S1) indicates that the self-assembly has promoted the *cis* to *trans* isomerization.<sup>40</sup> Transmission electron microscopy (TEM) images captured at different time scales reveal the programmed formation of hollow cone-shell structures (Figure 1C). Helical ribbons displaying both *M* and *P* chirality already formed after initial mixing (Figure C1), which coiled into rocket heads within 5 min (Figure C2). Ten min later, a structure with cone-shell morphology came into formation, with the diameter and length

around 200 and 600 nm (Figure C3), respectively. The cone shells kept growing with time, and the final length could be several micrometers (Figure C4). Scanning electron microscopy (SEM) images revealed the coexistence of both *M* and *P* helical coils, and their ratio is half-to-half (Figure C5), indicating that the pristine C4AZO- $\text{Zn}^{2+}$  self-assembly is racemic. Accordingly, no circular dichroism was detected (Figure 2C, upper panel, black curve). Elemental analysis (Table 1) suggests that the cone shells are composed of the electroneutral  $\text{Zn}(\text{C4AZO})_2$  compound. Since this compound is charge neutral and contains two hydrophobic C4AZO chains, it displays very strong self-assembling ability, which

**Table 1. Elemental Analysis (EA) Results of the C4AZO- $\text{Zn}^{2+}$  Aggregates<sup>a</sup>**

sample	method	C (wt %)	N (wt %)	H (wt %)
C4AZO- $\text{Zn}^{2+}$	theoretical	64.65	8.38	5.74
	experimental	62.99	8.15	5.84
C4AZO- $\alpha$ -CyD- $\text{Zn}^{2+}$	theoretical	49.25	2.13	6.06
	experimental	62.40	8.13	5.53

<sup>a</sup>Theoretical values are listed as a contrast.

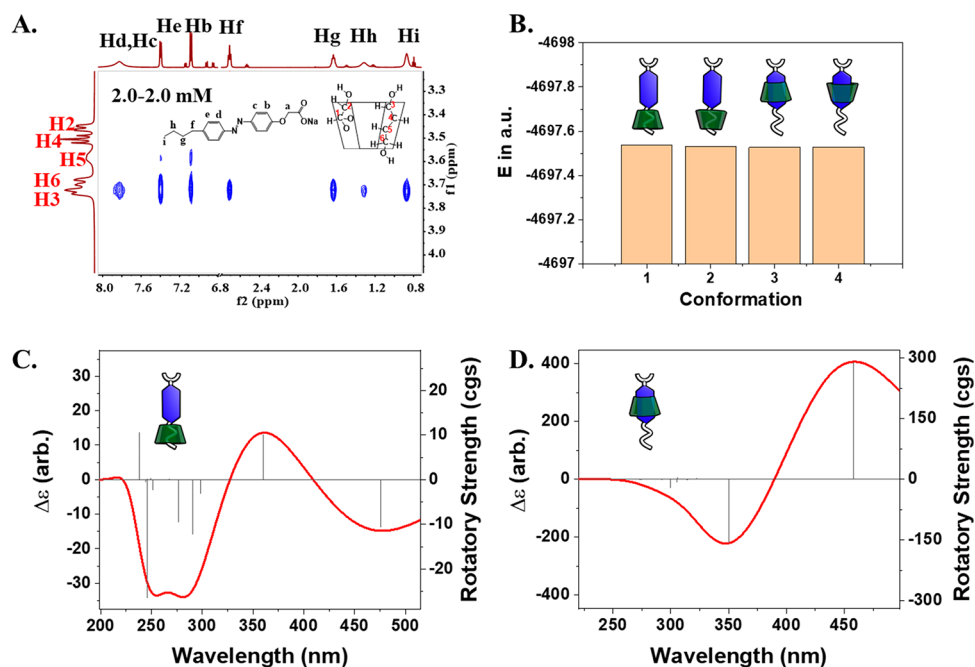


**Figure 3.** (A) 2D NMR (ROESY) spectra of the C4AZO/ $\alpha$ -CyD complexes (C4AZO/ $\alpha$ -CyD = 2:2 mM, and the peak attribution of  $\alpha$ -CyD was referred to in the literature<sup>43,44</sup>). (B) Geometry-optimized energies of different C4AZO/ $\alpha$ -CyD conformations based on DFT calculation. The sphere-stick models of the optimized conformations are shown in Figure S8. (C,D) DFT-calculated ICD spectra of the supramolecular chirality for the two conformations that C4AZO is threaded into  $\alpha$ -CyD from the narrower rim with different locations: (C)  $\alpha$ -CyD on the alkyl chain and (D)  $\alpha$ -CyD on the AZO.

coincides with the quick precipitation process in the system. X-ray photoelectron spectroscopy (XPS) measurements (Figure 1D) reveal that the O 1s of the COO<sup>−</sup> group displays two different binding energies in C4AZO, but only one energy occurs in Zn(C4AZO)<sub>2</sub>. Meanwhile, the binding energy of Zn<sup>2+</sup> 2p<sub>1/2</sub> and 2p<sub>3/2</sub> has decreased by 0.7 and 0.5 eV, respectively (Figure S4), indicating the COO<sup>−</sup> group interacted with Zn<sup>2+</sup> through a chelating mode, as illustrated by the inset in Figure 1D. This picture is further confirmed by Fourier transform infrared spectrum (FT-IR) measurements, which show that the separation between the asymmetric and symmetric vibration is decreased by 54 cm<sup>−1</sup>, namely, from 1604–1418 = 186 cm<sup>−1</sup> to 1564–1432 = 132 cm<sup>−1</sup> (Figure 1E).<sup>41,42</sup>

It is worth noting that the C4 chain is very crucial for the helical structure formation. As the C4 chain is removed or reduced to C2 (Figure S5), only flat plates were formed. This means that the C4 alkyl chains in the bilayers may protrude some steric hindrance for the stacking of the AZO groups in the Zn(C4AZO)<sub>2</sub>-coordinating self-assembly, so that they have to form some dislocation in packing during the assembly with Zn<sup>2+</sup>.

**Symmetry Breaking in the Cone Shells.** However, as the C4AZO was allowed to form a host–guest complex with  $\alpha$ -CyD at the molar ratio of 1:1 (Figure 2A and Figure S6, <sup>1</sup>H NMR, S7-MS), further addition of Zn<sup>2+</sup> led to drastic symmetry breaking in the cone-shell self-assemblies. Increasing the  $\alpha$ -CyD to C4AZO molar ratio to 2:1 or 3:1 could not form the cone shells. Figure 2B shows the SEM image of the predominant P-chiral cone shells formed in the 2 mM C4AZO/2 mM  $\alpha$ -CyD/1 mM Zn(NO<sub>3</sub>)<sub>2</sub> system. In line with this symmetry breaking in microstructures, the suspension displays a distinct chiral signal (Figure 2C, upper panel) corresponding to the UV absorbance of the AZO groups

(Figure 2C, lower panel). Elemental analysis (Table 1) reveals that the P-chiral cone shells have nearly the same composition as the racemic ones in Figure 1C. <sup>1</sup>H NMR measurements (Figure 2D) for the clean precipitates, after centrifugation from the supernatant, further confirm that  $\alpha$ -CyD does not exist in the P-chiral cone shells. However, the X-ray diffraction (XRD) peaks shift to smaller angles for the symmetry-breaking cone shells, and the diffractions are stronger (Figure 2E). According to the Bragg equation, 2D lamellar lattices were formed in both cases, but the thickness of the bilayers, determined from the 001 diffraction, is 3.07 nm in the racemic system, which is 0.6 nm shorter than the 2-fold fully extended length of C4AZO (Figure S8). It is noticed that 0.6 nm is exactly the length of the butyl chain (Figure S8). This means that the butyl chains have staggered in the bilayers in the racemic cone shells (inset in Figure 2E1, upper panel). However, the bilayer thickness for the  $\alpha$ -CyD-mediated cone shells increases to 3.33 nm, indicating that the two half-layers are more stretched (inset in Figure 2E1, lower panel). This different molecular packing in the racemic and symmetry-breaking cone shells manifests clearly that the host–guest interaction between C4AZO and  $\alpha$ -CyD has changed the self-assembling process of the Zn(C4AZO)<sub>2</sub> unit.

**Role of  $\alpha$ -CyD in the Symmetry Breaking.** To further understand the role of  $\alpha$ -CyD in the symmetry breaking, both 2D <sup>1</sup>H NMR measurements and theoretical calculations were performed to study the binding mode of  $\alpha$ -CyD with C4AZO and the predicted ICD spectra. It is amazing to find that both the H3 and H5,6 protons, which are on the wider and narrower rim of  $\alpha$ -CyD, respectively, have correlations with all the protons of C4AZO (Figure 3A). This means that  $\alpha$ -CyD does not have a preferred binding position and orientation on the C4AZO skeleton. The theoretical energies for the different host–guest supramolecular conformations based on quantum

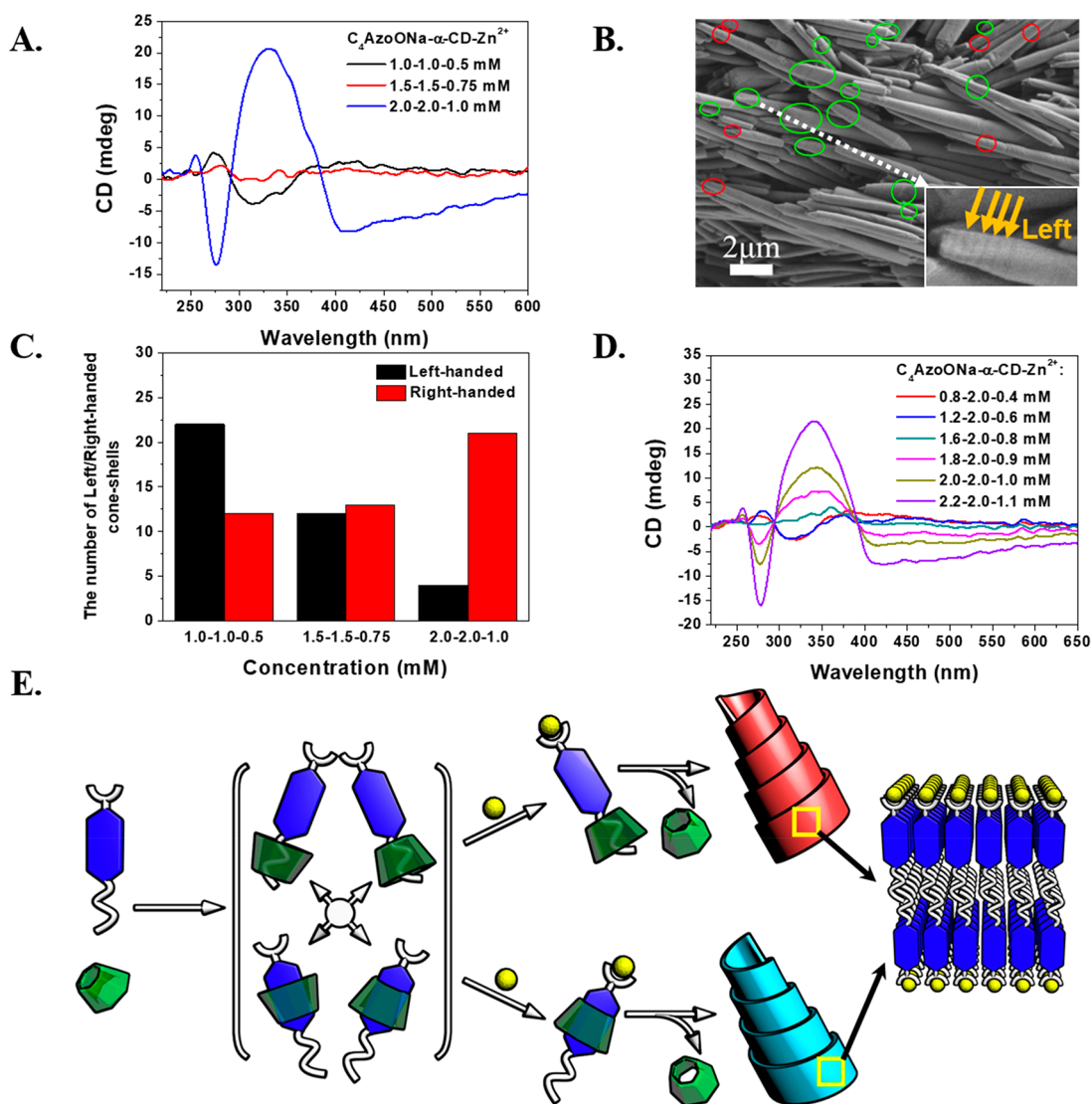


**Figure 4.** (A) CD spectra of C<sub>4</sub>AZO-α-CyD-Zn<sup>2+</sup> suspensions at a fixed molar ratio of 2:2:1 with increasing concentration of each component. (B) SEM images of the C<sub>4</sub>AZO-α-CyD-Zn<sup>2+</sup> aggregates at the concentration of 1.0:1.0:0.5 mM. The inset shows the enlarged view of the selected circle. (C) Statistic results of number of M/P-chiral cone shells from the SEM images (concentrations of 1.0:1.0:0.5 mM, 1.5:1.5:1.5 mM, and 2.0:2.0:1.0 mM). (D) CD spectra of C<sub>4</sub>AZO-α-CyD-Zn<sup>2+</sup> suspensions at the C<sub>4</sub>AZO/Zn<sup>2+</sup> molar ratio of 2:1 while increasing the relative ratio to α-CyD. (E) Proposed mechanism of α-CyD-catalyzed symmetry breaking in racemic cone-shell self-assemblies. The molecular packing in the bilayers is illustrated as the same mode for simplicity.

chemistry calculation are quite close (Figures 3B and S9), indicating they are all possible states. However, Figure 3C,D and Figure S10 reveal that the calculated ICD spectra for these host-guest complexes are distinctly different. As the butyl group is threaded into the cavity of α-CyD from the narrower rim (inset in Figure 3C), the ICD is negative at 260 and 450 nm but positive at 365 nm (Figure 3C). In contrast, as the AZO group is threaded into the cavity from the same direction, a negative ICD would occur at 365 nm and a positive one at wavelengths larger than 450 nm (Figure 3D). The DFT calculation suggests that these ICD peaks are from the electron transitions between molecular orbitals from different groups rather than the simple Cotton splitting effect. Detailed peak assignment is provided in Figure S10. Clearly, the ICD signal observed in Figure 2C for the 2 mM C<sub>4</sub>AZO-α-CyD-Zn system is in accordance with that for the ICD of C<sub>4</sub>AZO with its butyl group threading into the cavity of α-CyD from the narrower rim, namely, the situation described in Figure 3C.

This means that the ICDs of C<sub>4</sub>AZO induced by α-CyD have been left when the coordinating self-assembly of Zn(C<sub>4</sub>AZO)<sub>2</sub> occurs, leading to symmetry breaking in the cone shells.

To further confirm the above postulation, we decided to measure the host-guest dynamics-dependent ICD of the cone-shell self-assemblies since the host-guest dynamics has a great impact on the threading position of the guest in the cavity of α-CyD, which may reverse the ICD at properly designed host dynamics.<sup>30</sup> Both concentrations and host-to-guest ratios are effective protocols to achieve dynamic control.<sup>30</sup> In principle, at lower concentrations, the exchanging rate between the C<sub>4</sub>AZO molecules in and out of the α-CyD is slower, so that the C<sub>4</sub>AZO molecules have time to thread deeper in α-CyD. As a result, the AZO group would have a larger chance to stay in the cavity of α-CyD. With increasing concentration, the exchanging rate becomes faster, which favors a shallower threading of C<sub>4</sub>AZO, thus resulting in threading of the butyl group in α-CyD. This scenario is confirmed with concen-

tration-dependent  $^1\text{H}$  NMR measurements (Figure S11). At the lower concentration of 1 mM, the fraction of  $\text{CH}_3$  of the butyl group in the cavity of  $\alpha$ -CyD is about 0.77, whereas it increases to 0.88 at the higher concentration of 2 mM. According to the theoretical calculations, these two scenarios would generate a reverse ICD signal at 365 nm for the C4AZO–Zn cone-shell structures. Figure 4A shows that the ICD inversion for the cone shells indeed occurs as the C4AZO concentration varies from 1 to 2 mM, while the molar ratio between different molecules remains constant. The system with 1.5 mM C4AZO is ICD silent, suggesting that the positive and negative ICD signals may cancel each other at this concentration. UV–vis spectra are similar for the systems with different concentrations (Figure S12). In accordance with the concentration-triggered ICD inversion, SEM observations clearly manifest the occurrence of predominant M-chiral cone shells at the low concentration of 1.0 mM (Figure 4B and Figure S13), which is opposite to the P-chiral ones obtained at the higher concentration of 2.0 mM (Figure 2B and Figure S14). Along with our expectations, at the concentration of 1.5 mM, racemic cone shells were observed (Figure S15). Statistical analysis on the handedness variation in SEM images with increasing concentration is illustrated in Figure 4C.

Similarly, the host–guest dynamics can also be manipulated by varying the molar ratio between C4AZO and CyD since larger C4AZO ratios would accelerate the exchanging rate between the C4AZO inside the cavity and that outside the cavity, resulting in shifting of the threading position from the AZO to the butyl group. Accordingly, we would expect the ICD inversion from negative to positive at 365 nm. Figure 4D shows that as the molar fraction of C4AZO increases the handedness of the ICD signal for the cone-shell assemblies reverses as well, indicating the AZO groups locate inside the cavity of CyD at lower AZO fractions, whereas it is outside of the cavity of CyD at higher AZO fractions.

**Symmetry-Breaking Mechanism.** The excellent agreement between the theoretical prediction and the experimental results allows us to propose the symmetry-breaking mechanism in the present study. Originally, C4AZO may thread into  $\alpha$ -CyD with both butyl and AZO groups from both the wider and narrower rim, resulting in diversified conformations as illustrated in Figure 3B. Since the formation energy is not very different, these conformations are in dynamic equilibrium with each other. However, upon addition of metal ions, the conformation with the narrower rim close to the polar head becomes dominant since it may encounter smaller steric hindrance when they further pack into bilayers. Because the coordination also reduces the electrostatic repulsions between the C4AZO molecules, the  $\pi$ – $\pi$  stacking is promoted significantly. As a result,  $\alpha$ -CyD is squeezed out of the system, but leaving the induced chirality to the coordinating self-assembly of  $\text{Zn}(\text{C4AZO})_2$ , as illustrated in Figure 4E.

## CONCLUSION

In conclusion, we successfully achieved symmetry breaking in racemic cone shells by using  $\alpha$ -CyD as a chiral configuration catalyst, following coordination as the main driving force for the directional self-assembly of completely achiral molecules. The chiral cavity of  $\alpha$ -CyD may induce a chiral signal for the achiral guest C4AZO, and the induced chirality can be rationally manipulated by controlling the host–guest dynamics according to the predictions of Harata and Kodaka. Because

the two scenarios described by Harata–Kodada’s rule can be achieved by controlling the host–guest dynamics, the handedness of the coordinating self-assembly can be rationally manipulated. This work reveals that dynamic factors, such as concentration and molar ratio, can be very effective in determining the supramolecular chirality at mesoscales, which not only may be informative for creating symmetry breaking for supramolecular self-assemblies but also inspires the origin of supramolecular chirality in Nature.

## EXPERIMENTAL SECTION

**Characterizations.** The TEM images were taken on a JEM-2100 transmission electron microscope (JEOL, Japan, 200 kV). SEM measurements were performed using a Hitachi S4800 microscope at an acceleration voltage of 1.0 kV. The XPS spectra of samples were tested with an X-ray photoelectron spectrometer (AXIS-Supra). The crystal information of the assemblies was obtained by  $\text{Cu K}\alpha$  radiation in an X-ray diffractometer (XRD, RigakuDmax-2000X). The FT-IR spectra were measured with a Spotlight200 microscopic infrared spectrometer. An elemental analyzer (virioEL, Elemental Analysensysteme GmbH company) was used to measure the contents of C, H, and N elements. The UV–vis spectra were obtained with a spectrometer (Shimadzu, UV-1800) using a 1 mm quartz cell in the range of 200–650 nm with a step size of 0.5 nm. The CD and linear dichroism (LD) spectra of liquid and suspension samples were measured on a JASCOJ-810 spectrometer, and a 1 mm quartz cell was also used. The scanning speed was set as 200 nm/min; the response time was 1 s; the bandwidth was 1 nm; and the CD spectra were obtained after two scans.  $^1\text{H}$  NMR and 2D-NMR (ROESY) spectra were performed on a Bruker ARX 500 MHz spectrometer at room temperature. The mass spectra of precipitates of the assemblies were measured on a Bruker SolarixXR electrospray ionization mass spectrometer.

**Calculation Details.** All the vacuum structural optimizations, model construction of the C4AZO/ $\alpha$ -CyD inclusion complex, and frequency and ICD spectra calculations were carried out based on density functional theory (DFT) as implemented in Gaussian 16.<sup>45</sup> The functional used is B3LYP, and the basis set was 6-31g(d). The  $\alpha$ -CyD structure was obtained from the ChemSpider database. First, the structures of  $\alpha$ -CyD and C4AZO were optimized. Then, C4AZO was threaded into the cavity of  $\alpha$ -CyD, and four typical C4AZO@ $\alpha$ -CyD inclusion conformations were selected for structural optimization and energy calculation: the hydrophobic chain of C4AZO was threaded into the cavity of  $\alpha$ -CyD from the narrower rim and the wider rim; the AZO part was threaded into the cavity of  $\alpha$ -CyD from the narrower rim and the wider rim, respectively. Time-dependent density functional theory (TDDFT) is used to calculate 20 excited states with the lowest energies for each conformation. The calculated energies with four conformations were listed successively under the velocity representation. It should be noted that the Gaussian 16 output rotatory strength unit uses the centimeter-gram-second system (CGS), and the rotor strength unit was  $10^{-40}$  erg-esu-cm/Gauss.

**Data Analysis.** Based on the four DFT-optimized conformations, corresponding ICD spectra were mapped using the Multiwfn program, and the ICD spectra were expanded by Gaussian function under the velocity representation.<sup>45</sup> The ICD is simulated by *ab initio* calculations, and the theoretical model we used to clarify the relationship between calculated rotatory strength and molar extinction coefficient can be found in the SI.

## ASSOCIATED CONTENT

### Supporting Information

The Supporting Information is available free of charge at <https://pubs.acs.org/doi/10.1021/acsnano.1c06766>.

Theoretical model; UV–vis and  $^1\text{H}$  NMR spectra of C4AZO; TEM image; XPS spectra of the C4AZO– $\text{Zn}^{2+}$  assemblies; additional  $^1\text{H}$  NMR and ESI-MS character-

ization of C4AZO/ $\alpha$ -CyD complexes at different ratios and concentrations; additional calculated structures, energies, and ICD spectra for C4AZO/ $\alpha$ -CyD complexes; UV-vis spectra corresponding to CD spectra and additional SEM images for the C4AZO- $\alpha$ -CyD-Zn<sup>2+</sup> suspensions (PDF)

## AUTHOR INFORMATION

### Corresponding Authors

**Yun Yan** – Beijing National Laboratory for Molecular Sciences (BNLMS), State Key Laboratory for Structural Chemistry of Unstable and Stable Species, College of Chemistry and Molecular Engineering, Peking University, Beijing 100871, P. R. China; [orcid.org/0000-0001-8759-3918](https://orcid.org/0000-0001-8759-3918); Email: [yunyan@pku.edu.cn](mailto:yunyan@pku.edu.cn)

**Yunlong Xiao** – Beijing National Laboratory for Molecular Sciences (BNLMS), State Key Laboratory for Structural Chemistry of Unstable and Stable Species, College of Chemistry and Molecular Engineering, Peking University, Beijing 100871, P. R. China; Email: [xiaoyl@pku.edu.cn](mailto:xiaoyl@pku.edu.cn)

### Authors

**Wanwan Zhi** – Beijing National Laboratory for Molecular Sciences (BNLMS), State Key Laboratory for Structural Chemistry of Unstable and Stable Species, College of Chemistry and Molecular Engineering, Peking University, Beijing 100871, P. R. China

**Zhichen Pu** – Beijing National Laboratory for Molecular Sciences (BNLMS), State Key Laboratory for Structural Chemistry of Unstable and Stable Species, College of Chemistry and Molecular Engineering, Peking University, Beijing 100871, P. R. China

**Cheng Ma** – Beijing National Laboratory for Molecular Sciences (BNLMS), State Key Laboratory for Structural Chemistry of Unstable and Stable Species, College of Chemistry and Molecular Engineering, Peking University, Beijing 100871, P. R. China

**Kaerdun Liu** – Beijing National Laboratory for Molecular Sciences (BNLMS), State Key Laboratory for Structural Chemistry of Unstable and Stable Species, College of Chemistry and Molecular Engineering, Peking University, Beijing 100871, P. R. China

**Xuejiao Wang** – Beijing National Laboratory for Molecular Sciences (BNLMS), State Key Laboratory for Structural Chemistry of Unstable and Stable Species, College of Chemistry and Molecular Engineering, Peking University, Beijing 100871, P. R. China

**Jianbin Huang** – Beijing National Laboratory for Molecular Sciences (BNLMS), State Key Laboratory for Structural Chemistry of Unstable and Stable Species, College of Chemistry and Molecular Engineering, Peking University, Beijing 100871, P. R. China

Complete contact information is available at: <https://pubs.acs.org/10.1021/acsnano.1c06766>

### Author Contributions

<sup>#</sup>W.Z. and Z.P. contributed equally. Wanwan Zhi carried out most of the experiments and drafted this paper. Yunlong Xiao provided the suggestions for the theoretical calculations, and Zhichen Pu completed the specific calculations. Cheng Ma composed the cartoons of the assemblies. Kaerdun Liu and Xuejiao Wang helped with the methodology of the experi-

ments. Jianbin Huang helped to discuss and analyze the results. Yun Yan designed the work and wrote up the paper. All authors have given approval to the final version of the manuscript.

### Notes

The authors declare no competing financial interest.

## ACKNOWLEDGMENTS

The authors are grateful to the National Natural Science Foundation of China (Grant Nos. 91856120, 22172004, and 21972003) and the Beijing National Laboratory for Molecular Sciences (BNLMS) for financial support.

## REFERENCES

- (1) De Rossi, U.; Dähne, S.; Meskers, S. C. J.; Dekkers, H. P. J. M. Spontaneous Formation of Chirality in J-Aggregates Showing Davydov Splitting. *Angew. Chem., Int. Ed. Engl.* **1996**, *35*, 760–763.
- (2) Zhang, S.; Yang, S.; Lan, J.; Yang, S.; You, J. Helical Nonracemic Tubular Coordination Polymer Gelators from Simple Achiral Molecules. *Chem. Commun.* **2008**, 6170–6172.
- (3) Xue, S.; Meng, L.; Wen, R.; Shi, L.; Lam, J.; Tang, Z.; Li, B.; Tang, B. Unexpected Aggregation Induced Circular Dichroism, Circular Polarized Luminescence and Helical Assembly from Achiral Hexaphenylsilole (Hps). *RSC Adv.* **2017**, *7*, 24841–24847.
- (4) Palmans, A. R. A.; Vekemans, J. A. J. M.; Hikmet, R. A.; Fischer, H.; Meijer, E. W. Lyotropic Liquid-Crystalline Behavior in Disc-Shaped Compounds Incorporating the 3,3'-Di(Acylamino)-2,2'-Bipyridine Unit. *Adv. Mater.* **1998**, *10*, 873–876.
- (5) Palmans, A. R. A.; Meijer, E. W. Amplification of Chirality in Dynamic Supramolecular Aggregates. *Angew. Chem., Int. Ed.* **2007**, *46*, 8948–8968.
- (6) Aparicio, F.; Vicente, F.; Sánchez, L. Amplification of Chirality in N,N'-1,2-Ethanediybisbenzamidates: From Planar Sheets to Twisted Ribbons. *Chem. Commun.* **2010**, *46*, 8356–8358.
- (7) Micali, N.; Engelkamp, H.; van Rhee, P. G.; Christianen, P. C. M.; Scolari, L. M.; Maan, J. C. Selection of Supramolecular Chirality by Application of Rotational and Magnetic Forces. *Nat. Chem.* **2012**, *4*, 201–207.
- (8) Sorrenti, A.; Rodriguez-Trujillo, R.; Amabilino, D. B.; Puigmartí-Luis, J. Milliseconds Make the Difference in the Far-from-Equilibrium Self-Assembly of Supramolecular Chiral Nanostructures. *J. Am. Chem. Soc.* **2016**, *138*, 6920–6923.
- (9) Bisoyi, H. K.; Li, Q. Light-Directed Dynamic Chirality Inversion in Functional Self-Organized Helical Superstructures. *Angew. Chem., Int. Ed.* **2016**, *55*, 2994–3010.
- (10) Wang, H.; Bisoyi, H. K.; Li, B.-X.; McConney, M. E.; Bunning, T. J.; Li, Q. Visible-Light-Driven Halogen Bond Donor Based Molecular Switches: From Reversible Unwinding to Handedness Inversion in Self-Organized Soft Helical Superstructures. *Angew. Chem., Int. Ed.* **2020**, *59*, 2684–2687.
- (11) Wang, L.; Urbas, A. M.; Li, Q. Nature-Inspired Emerging Chiral Liquid Crystal Nanostructures: From Molecular Self-Assembly to DNA Mesophase and Nanocolloids. *Adv. Mater.* **2020**, *32*, 1801335.
- (12) Takashima, S.; Abe, H.; Inouye, M. Copper(Ii)/Phenanthroline-Mediated Cd-Enhancement and Chiral Memory Effect on a Meta-Ethynylpyridine Oligomer. *Chem. Commun.* **2012**, *48*, 3330–3332.
- (13) Yang, D.; von Krbek, L. K. S.; Yu, L.; Ronson, T. K.; Thoburn, J. D.; Carpenter, J. P.; Greenfield, J. L.; Howe, D. J.; Wu, B.; Nitschke, J. R. Glucose Binding Drives Reconfiguration of a Dynamic Library of Urea-Containing Metal–Organic Assemblies. *Angew. Chem., Int. Ed.* **2021**, *60*, 4485–4490.
- (14) Vera, F.; Tejedor, R. M.; Romero, P.; Barberá, J.; Ros, M. B.; Serrano, J. L.; Sierra, T. Light-Driven Supramolecular Chirality in Propeller-Like Hydrogen-Bonded Complexes That Show Columnar Mesomorphism. *Angew. Chem., Int. Ed.* **2007**, *46*, 1873–1877.

- (15) Hu, J.; Kuang, W.; Deng, K.; Zou, W.; Huang, Y.; Wei, Z.; Faul, C. F. J. Self-Assembled Sugar-Substituted Perylene Diimide Nanostructures with Homochirality and High Gas Sensitivity. *Adv. Funct. Mater.* **2012**, *22*, 4149–4158.
- (16) Ye, Q.; Zheng, F.; Zhang, E.; Bisoyi, H. K.; Zheng, S.; Zhu, D.; Lu, Q.; Zhang, H.; Li, Q. Solvent Polarity Driven Helicity Inversion and Circularly Polarized Luminescence in Chiral Aggregation Induced Emission Fluorophores. *Chem. Sci.* **2020**, *11*, 9989–9993.
- (17) Huang, X.; Li, C.; Jiang, S.; Wang, X.; Zhang, B.; Liu, M. Self-Assembled Spiral Nanoarchitecture and Supramolecular Chirality in Langmuir–Blodgett Films of an Achiral Amphiphilic Barbituric Acid. *J. Am. Chem. Soc.* **2004**, *126*, 1322–1323.
- (18) Chen, Q.; Chen, T.; Wang, D.; Liu, H.; Li, Y.; Wan, L. Structure and Structural Transition of Chiral Domains in Oligo(P-Phenylenevinylene) Assembly Investigated by Scanning Tunneling Microscopy. *Proc. Natl. Acad. Sci. U. S. A.* **2010**, *107*, 2769–2774.
- (19) Qiu, Y.; Chen, P.; Liu, M. Evolution of Various Porphyrin Nanostructures via an Oil/Aqueous Medium: Controlled Self-Assembly, Further Organization, and Supramolecular Chirality. *J. Am. Chem. Soc.* **2010**, *132*, 9644–9652.
- (20) Danila, I.; Riobé, F.; Piron, F.; Puigmartí-Luis, J.; Wallis, J. D.; Linares, M.; Ågren, H.; Beljonne, D.; Amabilino, D. B.; Avarvari, N. Hierarchical Chiral Expression from the Nano- to Mesoscale in Synthetic Supramolecular Helical Fibers of a Nonamphiphilic C3-Symmetrical  $\Pi$ -Functional Molecule. *J. Am. Chem. Soc.* **2011**, *133*, 8344–8353.
- (21) Guo, Z.; Yuan, J.; Cui, Y.; Chang, F.; Sun, W.; Liu, M. Supramolecular Assemblies of a Series of 2-Arylbenzimidazoles at the Air/Water Interface: *In Situ* Coordination, Surface Architecture and Supramolecular Chirality. *Chem. - Eur. J.* **2005**, *11*, 4155–4162.
- (22) Chen, Y.; Liu, Y. Cyclodextrin-Based Bioactive Supramolecular Assemblies. *Chem. Soc. Rev.* **2010**, *39*, 495–505.
- (23) Zhdanov, Y. A.; Alekseev, Y. E.; Kompantseva, E. V.; Vergeychik, E. N. Induced Optical-Activity in Cyclodextrin Complexes. *Usp. Khimii.* **1992**, *61*, 1025–1046.
- (24) Harata, K.; Uedaira, H. The Circular Dichroism Spectra of the  $\beta$ -Cyclodextrin Complex with Naphthalene Derivatives. *Bull. Chem. Soc. Jpn.* **1975**, *48*, 375–378.
- (25) Harata, K. Induced Circular Dichroism of Cycloamylose Complexes with Meta- and Para-Disubstituted Benzenes. *Bioorg. Chem.* **1981**, *10*, 255–265.
- (26) Kodaka, M.; Fukaya, T. Induced Circular Dichroism Spectrum of  $\alpha$ -Cyclodextrin Complex with Heptylviologen. *Bull. Chem. Soc. Jpn.* **1989**, *62*, 1154–1157.
- (27) Kodaka, M. Sign of Circular Dichroism Induced by  $\beta$ -Cyclodextrin. *J. Phys. Chem.* **1991**, *95*, 2110–2112.
- (28) Kodaka, M. A General Rule for Circular Dichroism Induced by a Chiral Macrocyclic. *J. Am. Chem. Soc.* **1993**, *115*, 3702–3705.
- (29) Pescitelli, G.; Di Bari, L.; Berova, N. Application of Electronic Circular Dichroism in the Study of Supramolecular Systems. *Chem. Soc. Rev.* **2014**, *43*, 5211–5233.
- (30) Wang, X.; Li, M.; Song, P.; Lv, X.; Liu, Z.; Huang, J.; Yan, Y. Reversible Manipulation of Supramolecular Chirality Using Host-Guest Dynamics between  $\beta$ -Cyclodextrin and Alkyl Amines. *Chem. - Eur. J.* **2018**, *24*, 13734–13739.
- (31) Krishnan, R.; Rakhi, A. M.; Gopidas, K. R. Study of  $\beta$ -Cyclodextrin–Pyromellitic Diimide Complexation. Conformational Analysis of Binary and Ternary Complex Structures by Induced Circular Dichroism and 2d Nmr Spectroscopies. *J. Phys. Chem. C* **2012**, *116*, 25004–25014.
- (32) Nonaka, K.; Yamaguchi, M.; Yasui, M.; Fujiwara, S.; Hashimoto, T.; Hayashita, T. Guest-Induced Supramolecular Chirality in a Ditopic Azoprobe–Cyclodextrin Complex in Water. *Chem. Commun.* **2014**, *50*, 10059–10061.
- (33) Wang, Y.; Lin, H.; Ding, S.; Liu, D.; Chen, L.; Lei, Z.; Fan, F.; Tian, Z. Some Thoughts About Controllable Assembly (I) — From Catalysis to Cassemblysis. *Zhongguo Kexue: Huaxue* **2012**, *42*, 525.
- (34) Zhao, J.; Wang, J.; He, W.; Ruan, Y.; Jiang, Y. Isolable Chiral Aggregates of Achiral  $\Pi$ -Conjugated Carboxylic Acids. *Chem. - Eur. J.* **2012**, *18*, 3631–3636.
- (35) Wang, Y.; Lin, H.; Chen, L.; Ding, S.; Lei, Z.; Liu, D.; Cao, X.; Liang, H.; Jiang, Y.; Tian, Z. What Molecular Assembly Can Learn from Catalytic Chemistry. *Chem. Soc. Rev.* **2014**, *43*, 399–411.
- (36) Lauerer, R.; Raudino, A.; Scolari, L. M.; Micali, N.; Purrello, R. From Achiral Porphyrins to Template-Imprinted Chiral Aggregates and Further. Self-Replication of Chiral Memory from Scratch. *J. Am. Chem. Soc.* **2002**, *124*, 894–895.
- (37) Song, T.; Liang, H. Synchronized Assembly of Gold Nanoparticles Driven by a Dynamic DNA-Fueled Molecular Machine. *J. Am. Chem. Soc.* **2012**, *134*, 10803–10806.
- (38) Wang, Y.; Sun, Y.; Shi, P.; Sartin, M. M.; Lin, X.; Zhang, P.; Fang, H.; Peng, P.; Tian, Z.; Cao, X. Chaperone-Like Chiral Cages for Catalyzing Enantio-Selective Supramolecular Polymerization. *Chem. Sci.* **2019**, *10*, 8076–8082.
- (39) Song, X. D.; Perlstein, J.; Whitten, D. G. Supramolecular Aggregates of Azobenzene Phospholipids and Related Compounds in Bilayer Assemblies and Other Microheterogeneous Media: Structure, Properties, and Photoreactivity. *J. Am. Chem. Soc.* **1997**, *119*, 9144–9159.
- (40) Wu, Z.; Xue, R.; Xie, M.; Wang, X.; Liu, Z.; Drechsler, M.; Huang, J.; Yan, Y. Self-Assembly-Triggered Cis-to-Trans Conversion of Azobenzene Compounds. *J. Phys. Chem. Lett.* **2018**, *9*, 163–169.
- (41) Deacon, G. B.; Phillips, R. J. Relationships between the Carbon-Oxygen Stretching Frequencies of Carboxylate Complexes and the Type of Carboxylate. *Coord. Chem. Rev.* **1980**, *33*, 227–250.
- (42) Qiao, Y.; Lin, Y.; Wang, Y.; Yang, Z.; Liu, J.; Zhou, J.; Yan, Y.; Huang, J. Metal-Driven Hierarchical Self-Assembled One-Dimensional Nanohelices. *Nano Lett.* **2009**, *9*, 4500–4504.
- (43) Tomatsu, I.; Hashidzume, A.; Harada, A. Cyclodextrin-Based Side-Chain Polyrotaxane with Unidirectional Inclusion in Aqueous Media. *Angew. Chem., Int. Ed.* **2006**, *45*, 4605–4608.
- (44) Rekharsky, M. V.; Goldberg, R. N.; Schwarz, F. P.; Tewari, Y. B.; Ross, P. D.; Yamashoji, Y.; Inoue, Y. Thermodynamic and Nuclear Magnetic Resonance Study of the Interactions of  $\alpha$ - and  $\beta$ -Cyclodextrin with Model Substances: Phenethylamine, Ephedrine, and Related Substances. *J. Am. Chem. Soc.* **1995**, *117*, 8830–8840.
- (45) Lu, T.; Chen, F. Multiwfn: A Multifunctional Wavefunction Analyzer. *J. Comput. Chem.* **2012**, *33*, 580–592.